Review

J. Astrophys. Astr., Vol. 36, No. 4, December 2015, pp. 495–511

Multicomponent Analysis of the UV Si IV and C IV Broad Absorption Troughs in BALQSO Spectra: The Examples of J01225+1339 and J02287+0002

D. Stathopoulos[1,2,*], E. Danezis[1], E. Lyratzi[1,2], A. Antoniou[1] & D. Tzimeas[1]

[1]*Department of Astrophysics, Astronomy and Mechanics, Faculty of Physics, University of Athens, Panepistimioupoli, Zographou 157 84, Athens, Greece.*
[2]*Eugenides Foundation, 387 Sygrou Av., 175 64, Athens, Greece.*
[*]*e-mail: dstatho@phys.uoa.gr*

Received 5 July 2015; accepted 24 September 2015
DOI: 10.1007/s12036-015-9359-4

Abstract. Broad Absorption Line QSOs (BALQSOs) are a subtype of radio-quite QSOs that exhibit complex and unusually broad (FWHM $\geq$ 2,000 km/s) absorption lines. The existence of these lines in BALQSO spectra raises some questions with respect to the properties, the physical conditions and kinematics of the BAL material as well as the morphology of BAL troughs. In this study, taking into consideration the clumpy structure of the AGN outflow winds, we propose a physical model in order to explain the formation of BAL troughs and we give the mathematical description of this model. We also propose a method for analyzing spectroscopically the BAL profiles in the UV region of the electromagnetic spectrum. This method consists of the criteria we set during the fitting process of BAL troughs. The purpose of these criteria is to enable us to determine the exact number of components needed to simulate accurately the BAL troughs and guarantee the uniqueness of the fit. We give an application of the model and the method for Si IV and C IV resonance lines in the case of two BALQSOs. From the analysis, we conclude that the BAL material is in the form of clouds (density enhancements) that move radially and intercept the line-of-sight to the central continuum source. Using our method, we find the number of absorption components needed to simulate the BAL profiles, which means the number of clouds in the line-of-sight. We calculate the velocity shifts, the FWHM and the optical depths of the absorption components of BALs and we propose an internal structure for these clouds. Finally, we give some correlations between the properties of absorption components of Si IV and C IV.

Key words. Broad absorption line quasars—absorption lines.

1. Introduction

Broad absorption line QSOs (BALQSOs) are a subtype of radio-quiet QSOs defined by the presence of deep, broad and high velocity absorption lines that are usually blueshifted with respect to the corresponding emission lines in the UV region of the electromagnetic spectrum (though there are cases that redshifted absorption has been observed, see Hall *et al.* (2013)). These broad absorption features are found in about 10–20% of the total quasar population (Foltz *et al.* 1990; Hewett & Foltz 1784; Reichard *et al.* 2003).

In general, Broad Absorption Lines (BALs) are complex and unusually broad absorption troughs which appear remarkably smooth in high resolution spectra. A wide range of absorption characteristics in terms of outflow velocity, level of ionization, structure of absorption troughs and strength of the absorption are revealed in the studies of BALQSOs. Outflow velocities usually range from 0–5,000 km/s up to 10,000–30,000 km/s while extreme cases where outflow reaches ∼60,000 km/s (Foltz *et al.* 1983) have been observed. The structure of absorption troughs ranges from very smooth (P-Cygni like where single trough absorption which begins very near zero outflow velocity is observed) for either shallow or deep absorption to very broken-up for either strong or weak absorption (Turnshek 1988). There are BALQSOs that have multiple trough absorption which sets in near zero outflow velocity while others show BAL troughs detached (∼20% of the time (Turnshek *et al.* 1988) from the emission peak not setting in until outflow reaches a velocity of 3,000–5,000 km/s).

For BALs, a representative line width is ∼10,000 km/s. However BALs exhibit considerable diversity among their profiles. The minimum requirements for classification as BAL are: velocity widths >2,000 km/s (Weymann *et al.* 1991) and blueshifted velocity extrema >5,000 km/s. However these values depend on how BAL troughs are defined. For example, the balnicity index (Weymann *et al.* 1991) which is applied in C IV, accounts only for troughs wider than 2,000 km/s and blueshifted more than 3,000 km/s. On the other hand, the absorption index (Trump *et al.* 2006), which can be used for any transition, is less restrictive and includes troughs no smaller than 1,000 km/s, which can set in near zero outflow velocity.

BALs clearly identify high velocity outflows (or inflows if the BAL troughs are redshifted with respect to the corresponding emission line) launched from a rotating accretion disc that surrounds and feeds the central black hole. The properties of the BAL material in phase space are uncertain. There may be a smooth, continuous flow (Murray & Chiang 1995) or many individual clouds. So a smooth absorption may be caused by a smooth continuous flow with the intensity depending only on optical depth effects (complete source coverage), or it may be due to a flow of many individual clouds (McKee & Tarter 1975; Turnshek 1984; Lyratzi *et al.* 2009, 2010, 2011; Hamann *et al.* 2013; Capellupo *et al.* 2014) which are optically thick and very small compared with the size of the central continuum source. According to the second point of view, the broad and complex absorption profiles can be interpreted as the synthesis of a series of absorption components. The absorbing regions can be thought as overdensities or density enhancements in the wind or interacting with the wind (Weymann *et al.* ; Filiz Ak *et al.* 2012), produced by the accretion disc and propagate radially at some angle above an optically thick torus (Murray *et al.* 1995; Elvis 2000; Proga *et al.* 2000). It is commonly accepted that the region producing

BALs (Broad Absorption Line Region – BALR) lies outside the region that produces Broad Emission Lines – BELs (Broad Emission Line Region – BELR).

Recent radiation-MHD simulations by Takeuchi *et al.* (2013) reproduce variable clumpy structures for the wind with typical sizes of $\sim$20 rg in warm absorbers, corresponding to $\sim 5 \times 10^{-4}$ pc assuming the black-hole mass of SDSS J1029+2623, MBH $\sim 108.72 M_{\odot}$. Furthermore, Misawa *et al.* (2014) succeeded in resolving the clumpy structure of the outflow winds in the gravitationally lensed quasar SDSS J1029+2623. Through their observations they rejected the hypothesis of a smooth homogenous outflow and concluded to complex small structures inside outflows from the galactic nucleus. They proposed two different structures for the clumpy outflow: (a) small gas clouds close to the flux source and (b) filamentary (or sheet-like) structure made of multiple clumpy gas clouds. Additionally, Filiz Ak *et al.* (2012) found that about three per cent of quasars of their sample show disappearing gas clouds over a three-year span, which in turn suggests that a typical quasar cloud spends about a century along our line-of-sight. They point out: "One potential implication of the observed frequency of disappearing C IV BAL troughs is a relatively short average trough rest-frame lifetime. Note that by lifetime we mean the time over which a trough is seen along our line-of-sight and not necessarily the lifetime of the gas clouds responsible for the absorption."

In the cloud picture, the primary agent responsible for a line's FWHM was supposed to be the macroscopic ordered motion of the gas, while the intrinsic line width was supposed to be due to thermal motions only. So the observed large widths of BALs are assumed to be due to bulk motions of clouds, or macrotrubulence (Gonçalves *et al.* 2001). If this holds, then it implies an extremely large number of clouds that are needed to create the smooth profiles. In the case of Broad Emission Lines (BELs), this number is about 10^7–10^8 (Arav *et al.* 1997, 1998; Dietrich *et al.* 1999). However, Bottorff *et al.* (2000), in order to give an answer to this conundrum introduced the effect of microturbulence in order to explain the great width of BELs and constrain the number of clouds. Furthermore, Bottorff & Ferland (2000) proposed that the line widths of contributing clouds or flow elements are much wider than their thermal widths, because of the presence of non-dissipative magneto-hydrodynamic waves. The collective contribution of clouds produces emission-line profiles broader and smoother than would be expected if a magnetic field were not present. According to previous researchers, smoothness can be achieved for less than $\sim 8 \times 10^4$ clouds which may even be as low as a few hundred. In another work, Bottorff & Ferland (2002) succeeded in reproducing the emission line spectrum, produced by emitting clouds, with a turbulent velocity of 200 km/s. Their assumption is that due to dissipative heating, the turbulent velocity field broadens the emission contributions of individual line-emitting clouds so that they overlap, smoothing the line profile.

According to the transitions observed, BALQSOs can be separated into the following categories: The first category includes the so called HiBALAQSOs (high ionization BALQSOs) where absorption appears in high level of ionization. The transitions which are dominant are C IV, N V, O VI. Also, moderate to weak absorption lines of transitions such as Si IV and Ly-α are observed. In the case of low ionization BALQSOs (LoBALQSOs, see Voit *et al.* (1993) and Gibson *et al.* (2009)), the absorption also has low ionization components and transitions of Mg II and sometimes C II are present. Other weak to intermediate strength transitions include Al III and C III.

LoBALQSOs are generally identified as BALs by the Mg II λ 2798 Å line profile. The last category includes the so-called FeLoBALs (Hazard *et al.* 1987), which, in addition to the above mentioned transitions, show broad absorption troughs in lowly ionized iron (e.g., Fe II, Fe III). According to the standard unification model, the difference between the AGN subtypes is the observers viewing angle towards the central engine (Elvis 2000). On the other hand, an alternative assumption is that LoBALQSOs are an evolutionary stage of AGN, in which the nucleus expels a surrounding dusty cocoon (Voit *et al.* 1993; Urrutia *et al.* 2009; Farrah *et al.* 2010, 2012).

Taking into consideration the observations of Misawa *et al.* (2014) that confirm the existence of clouds, in this paper, we propose a physical and mathematical model able to analyze the complex structure of Si IV and C IV BAL profiles. Furthermore, by analyzing the Si IV and C IV BALs we try to answer the following questions: How can someone constrain the number of components needed to reproduce the Si IV and C IV BAL profiles and thus be sure not only for the goodness but also for the uniqueness of the fit? What are the physical and kinematical properties of the BAL material? Are there any correlations between the Si IV and C IV BALs?

This paper is structured as follows: In section 2, we describe the proposed physical model and the mathematical expression of the model. In section 3, we give the criteria under which we perform multicomponent fits to the Si IV and C IV broad absorption troughs. We also describe the line and continuum fitting as well as the goodness of fit and error analysis. In section 4, we apply the method in the case of two BALQSOs and in section 5, we present our results. Finally, in section 6, we discuss the implications and conclusions of our analysis.

2. Physical model

Broad Absorption Lines (BALs) are strong and unusually broad absorption troughs which appear remarkably smooth in high resolution spectra. BAL profiles can not be simulated by a single known distribution (e.g. Gauss, Lorentz, Voigt etc). Because of this characteristic, it has been proposed that BALs consist of a series of absorption components produced by density enhancements called clouds (McKee & Tarter 1975; Turnshek 1984; Lyratzi *et al.* 2009, 2010, 2011; Filiz Ak *et al.* 2012; Hamann *et al.* 2013; Capellupo *et al.* 2014; Misawa *et al.* 2014). Clouds, which are the core of this study, intercept the line-of-sight and are moving radially, exhibiting negligible rotation.

The components we use in order to simulate the BAL profiles correspond to clouds (Regions I, Fig. 1) and they are broad (120 km/s $<$ FWHM $<$ 2200 km/s) compared to the thermal and microturbulent width. For example, for Si IV the thermal width in 10^4 K gas is FWHM $\sim$ 4 km/s and for a gas of 10^5 K, FWHM $\sim$ 12 km/s. For C IV, these values are about 6 km/s and 20 km/s respectively. As for the microturbulent velocities these range from tenths of km/s to a few hundred, though Bottorff *et al.* (2000) showed that a microturbulent velocity of 10^3 km/s does not violate observations in the case of broad emission lines. So the thermal and microturbulent widths are too small compared to the widths of the components we use in the fits. In order to explain this discrepancy, we propose that what we call clouds are clusters of subunits called cloud elements or cloudlets (cloud elements – regions II, Fig. 1). To avoid confusion, we will always refer to the larger, more distinct structures as 'clouds'

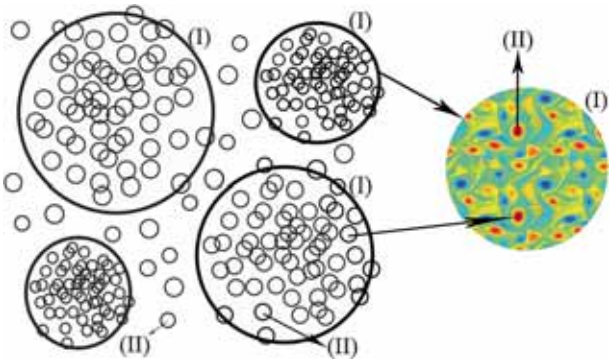

Figure 1. Representation of clouds (I) and cloudlets (II). The cloudlets are assumed to form clusters and each cluster is called a cloud.

(Regions I, Fig. 1) and the smaller structures as 'cloud elements' or cloudlets. We borrow the term 'cloud elements' from Bottorff & Ferland (2001). According to them, each BLR cloud is a collection of overlapping constant density clumps and these smallest clumps are called cloud elements.

Each cloudlet produces an absorption line, the width of which depends on thermal and microturbulent motions of ions inside the cloudlet. The synthesis of all these cloudlet lines that are very close in velocity space and overlap, produce a broad component corresponding to a cloud.

2.1 *Mathematical expression of the model*

The mathematical model is built on the basis that the BALR/BELR consists of a number of absorbing/emitting clouds that intercept the line-of-sight towards the central regions of the QSO that produce the continuum radiation (Lyratzi *et al.* 2007). The clouds, for modeling reasons are assumed to be spherically symmetric around their own centers. The observed BALs/BELs are the synthesis of absorption/emission components produced by these clouds. So, in order to conclude to a mathematical function, that can simulate the complex BAL/BEL profiles produced by clouds, Danezis *et al.* (2003) solved the radiative transfer equation for such a complex plasma region. The final equation derived by the solution of radiative transfer is

$$I_\lambda = \left[I_{\lambda 0} \prod_i \exp\{-L_i \xi_i\} + \sum_j S_{\lambda ej} (1 - \exp\{-L_{ej} \xi_{ej}\}) \right] \prod_g \exp\{-L_g \xi_g\}, \quad (1)$$

where i is the number of absorbing clouds in the line-of-sight, j is the number of emitting clouds in the line-of-sight, g is the number of additional absorbing clouds that may cover the i absorbing clouds as well as the j emitting clouds, $I_{\lambda 0}$ is the initial radiation intensity $\prod_i \exp\{-L_i \xi_i\}$ is the factor that describes the synthesis of absorption components produced by i clouds, $\sum_j S_{\lambda_{ej}} (1 - \exp(L_{ej} \xi_{ej}))$ is the factor that describes the synthesis of emission components produced by j clouds, $\prod_g \exp\{-L_g \xi_g\}$: is the factor that describes absorbing clouds that obscure both the i

absorbing as well as the j emitting clouds, L_i, L_{ej}, L_g are the distribution functions of the absorption coefficients $k_{\lambda i}$, $k_{\lambda ej}$, $k_{\lambda g}$, $k_{\lambda i}$ is the absorption coefficient of the i-th cloud in the line-of-sight, $k_{\lambda ej}$ is the absorption coefficient of the j-th emission cloud in the line-of-sight, $k_{\lambda g}$: is the absorption coefficient of the additional absorbing clouds that may cover the i and j clouds in the line-of-sight, ξ is the optical depth (τ) at the center of the spectral line and $S_{\lambda ej}$ is the source function, that is constant during one observation.

The geometry of the model is included in the factors L (Lyratzi *et al.* 2007; Danezis *et al.* 2007), of equation (1). After investigating a number of geometries for the clouds we concluded that the best fit of absorption/emission lines is accomplished if the geometry is spherical (Danezis 1983; Bates & Gilheany 1990; Gilheany *et al*. 1990; Waldron *et al*. 1992; Rivinius *et al*. 1997; Markova 2000). Apart from the geometry, the parameters 'L' can take the expression of one of the following distributions, according to the physical conditions we like to describe. So L can take the form of either Gauss (random motions – thermal and non thermal), or Lorentz (pressure), or Voigt (random motions and pressure), or rotation (rotation of a region around its own center, Danezis *et al.* 2003, 2007), or Gauss – rotation (random motions and rotation of a region around its own center (Danezis *et al.* 2003, 2007)).

2.2 *Use of equation* (1)

During the fitting process we use equation (1) independently for every component of a doublet. For example in the case of C IV λλ 1548.187, 1550.772 Å, we apply equation (1) twice, once for the 1548.187 Å (blue) and once for the 1550.772 Å (red) components of the doublet. By applying equation (1) twice we get two sets of lines. The first one contains all the blue components of C IV doublet (in Fig. 2 in the case of J01225+1339, there are 11 blue components, 9 absorption and 2 emission), while the second one contains all the red components of C IV doublet (in Fig. 2, there are 11 red components, 9 absorption and 2 emission). Having these two sets of lines, we then synthesize them to get the best fit. In the case of absorption lines, we use Gauss distribution while in the case of emission lines, we use Voigt distribution.

3. Fitting criteria

When fitting broad absorption troughs we encounter two major problems: Not only are we concerned about the best fit but also for the uniqueness of it. This means that we do not search just for the best fit but we want to be sure that the number of components and the values of the parameters used are uniquely determined. Before moving to the fitting criteria we would like to point out the following:

– We choose to fit resonance lines and not singlets because in the case of singlets we cannot constrain the number of components that gives the best fit of an absorption/emission profile. In the case of singlets, the more the components the better the fit.
– We do not treat resonance lines as singlets but instead we treat each member of a doublet independently. Treating doublets as singlets, is an oversimplification, that can lead to large deviation in the values of measured parameters, especially in the

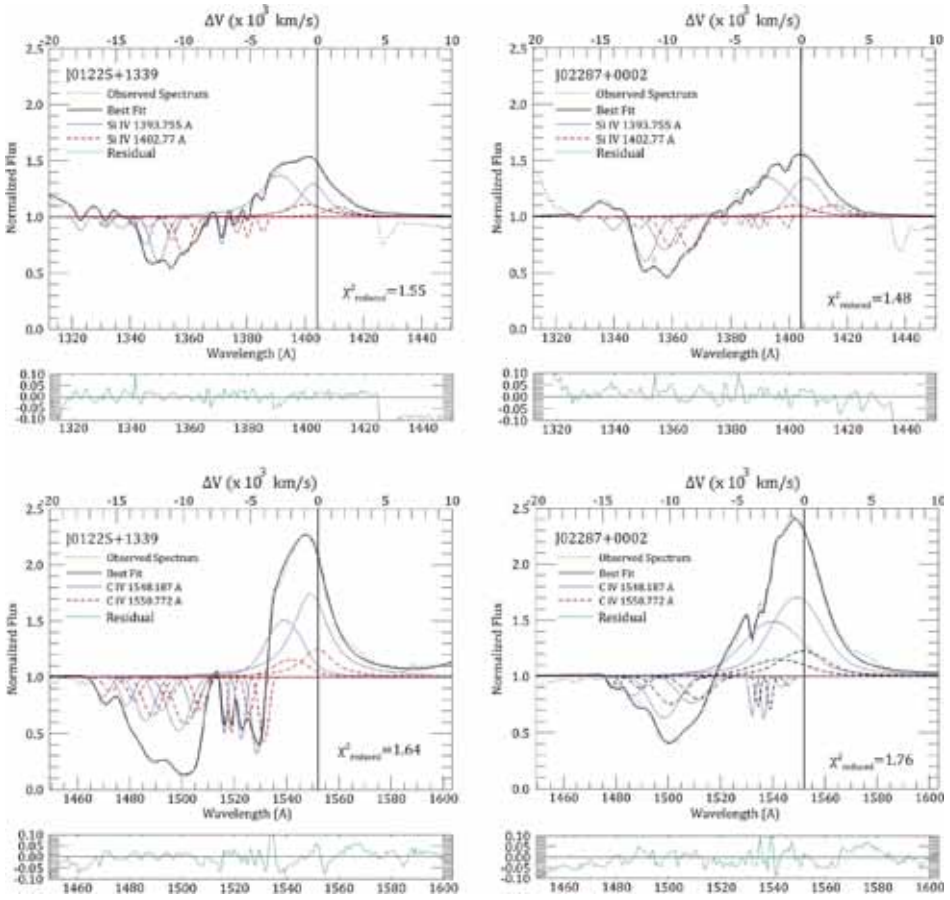

Figure 2. Best fits of the Si IV and C IV spectral regions of J01225+1339 and J02287+0002. The black dotted line denotes the observed spectrum while black, thick solid line corresponds to the best fit. We denote the shorter wavelength member of a doublet with blue thin solid line (blue: 1393.755 Å for Si IV and 1548.187 Å for C IV) while we denote the longer wavelength member of a doublet with the red dashed line (red: 1402.77 Å for Si IV and 1550.772 Å for C IV). The zero velocity corresponds to the longer wavelength member of a doublet. Below each fit we present a panel with the residual, which appears in green thin line. Furthermore, the reduced χ^2 is given for every fit. Note that the value of the reduced χ^2 serves only as a qualitative measure of the fit and should not be interpreted as indicating the probability of the fit.

case of Si IV where the wavelength separation between the blue and red components is large. Furthermore treating doublets as singlets prevents us from applying the criteria that follow. By using equation (1) twice we study independently the blue and red component of a doublet.

– The number of components needed to reproduce a broad absorption trough is controversial and probably will remain an open question for a long time. The major problem of multicomponent fits is that the best-fit solution is not unique (Laor *et al.* 1994). In the case of the UV Si IV and C IV resonance lines, their doublets are

blended. This means that the fit will be highly degenerate unless both ions are fitted simultaneously. So in order to find a final solution, which is unique, and independent of initial parameter/guess we fit simultaneously Si IV and C IV doublets with parameters tied. We assume that both Si IV and C IV follow the same kinematic structure (Becker *et al.* 2009).

From all of the above, we conclude to two groups of criteria:

(1) Criteria between the blue and red components of a doublet (C IV λλ 1548.187, 1550.772 Å and Si IV λλ 1393.755, 1402.77 Å).

(a) The number of blue and red components of a doublet must be exactly the same. This means that to each component of the 1548.187 Å C IV line corresponds a component of the 1550.772 Å C IV line. The same applies to the Si IV doublet.
(b) Each C IV 1548.187 Å component at a specific velocity shift has its corresponding C IV 1550.772 Å component at the same velocity shift. The same applies to the Si IV doublet. However, we require that the difference in velocities at line center must not differ from the expected doublet separation by more than one velocity bin (this condition is adopted from Wildy *et al.* (2015)). In the spectra studied in this paper, one velocity bin corresponds to ∼120 km/s.
(c) The C IV 1548.187 Å component and C IV 1550.772 Å component at the same velocity shift must have the same width. The same applies to the Si IV doublet. The components' FWHM cannot be smaller than the spectrograph's FWHM, which sets an upper limit on the number of components required to achieve the best fit.
(d) For emission lines, the ratio of optical depths between the blue and the red component is $\tau_b/\tau_r = 2$, as dictated by atomic physics (Savage & Sembach 1991). For absorption lines this ratio is free to vary $1{:}1 \leq \tau_b/\tau_r \leq 2{:}1$.

(2) Criteria between C IV and Si IV components at the same outflow velocity from the corresponding emission redshift.

(a) Both C IV and Si IV doublets consist of the same number of components.
(b) Each C IV 1548.187 Å (blue) component at a specific velocity shift has its corresponding Si IV 1393.755 Å (blue) component at the same velocity shift. The same applies between the C IV 1550.772 Å (red) components and the Si IV 1402.77 Å (red) components. In practice, Si IV absorption components are shallower than the ones appearing in C IV. So, there is the possibility that a very shallow C IV component has the corresponding Si IV at the same outflow velocity which possibly is not detectable.
(c) τ_b/τ_r(C IV) at a specific velocity shift must be the same as τ_b/τ_r (Si IV) at the same velocity shift. This criterion is applied under the assumption that both doublets (Si IV and C IV) at the same velocity offset are formed in the same outflow and that the physical conditions do not change significantly as a function of velocity (de Kool *et al.* 2002).

We point out that the fitting code is forced to fulfil all the criteria mentioned above. So these criteria are in fact the constrains that are followed during the fitting process and they are not set in order to cross check our results in the end.

3.1 *Line, continuum fitting and goodness of fit*

The continuum fit: For the continuum we fit a power law model to a set of continuum windows free of strong emission lines using the Levenberg–Marquardt minimization process. These windows are: 1320–1340 Å, 1445–1465 Å, 1700–1705 Å, 2155–2200 Å.

The line-fitting: Curve fitting is the process of constructing a curve or mathematical function, which has the best fit to a series of data points such as the BALQSOs spectra under study. Curve fitting involves interpolation where an exact fit to the data is required.

In our analysis, from a mathematical point of view, we are looking for the mathematical function (equation (1)) which, under specific constraints (criteria 1 and 2), when interpolated will give us the best fit to the data. We need to mention that our model does not give a least square fit to the data. Instead we iterate until the operator is satisfied that the data are satisfactory modeled. Data are assumed to be satisfactory modeled when we get a reduced χ^2 smaller than two. As mentioned in section 2.1.1, the final mathematical function that we interpolate in a spectral region is the synthesis of as many functions (equation (1)) as the lines under study (e.g. for S IV 1393.755, 1402.77 Å, we combine two functions, one for the blue line and one for the red line, where the first function describes the synthesis of all the 1393.755 Å components and the second describes all the 1402.77 Å components).

From a physical point of view, the best fit depends on the values that the parameters of equation (1) can take. These values must be subject to the constraints that the criteria (1) and (2) set.

In order to find the best fit, we increase the number of doublets until a standard F-test yields no further significant gain (95% confidence level) in the goodness of fit, as measured by the reduced χ^2.

We remind that in the case of absorption lines we use Gauss distribution while in the case of emission lines we use Voigt distribution.

3.2 *Error analysis*

The uncertainties of absorption line fitting parameters are estimated by adding Gaussian noise to the best fits. The width of the Gaussian at each pixel equals the flux uncertainty at that pixel. For each best fit, we produce 60 noisy spectra and fit each one of them in the same manner we fit the original spectrum. The uncertainty of each spectral parameter is then measured from its distribution. The error bar of a spectral parameter is then calculated as the RMS of 60 fitting results.

4. Application in BALQSOs J01225+1339 and J02287+0002

In order to test our method we give an application in the case of two BALQSOs: J01225+1339 and J02287+0002. The data were obtained between Nov. 2006 and Jan. 2007 using the VLT2/FORS1 telescope operated in service mode. FORS1 is the visual and near UV focal reducer and low dispersion spectrograph (300 V grism of 11.1 Å FWHM) of the Very Large Telescope (VLT) operated by European Southern Observatory (ESO) (Appenzeller *et al.* 1998). The BALQSO J01225+1339 has a redshift of 3.0511 and a signal to noise ratio (S/N) of 92 in the continuum around 1700 Å, while the redshift of J02287+0002 is 2.7282 and S/N is 67. For more information about the data, see Negrete *et al.* (2014).

Because this study focusses on the characteristics of and differences between C IV and Si IV BAL troughs in corresponding velocity ranges, we adjust the maximum blue edge velocity limit of the C IV BAL trough region considering the Si IV region. Usually the Si IV region is blended with the emission lines of O I 1302 Å (at $\simeq -21,800$ km/s from Si IV emission), Si II 1304 Å (at $\simeq -21,300$ km/s from Si IV emission), C II 1334 Å (at $\simeq -14,500$ km/s from Si IV emission). These emission lines are usually weak; however by visually inspecting the spectra, we observed that in some cases these weak features may affect the Si IV BAL troughs. Thus we consider that a BAL trough extends up to $-20{,}000$ km/s following Filiz Ak *et al.* (2014).

5. Results

In Fig. 3, we present the continuum fits to the spectra of both BALQSOs, while in Fig. 2 we give detail of the best fits of Si IV and C IV spectral regions as well as the individual components that compose the final profiles. We present the values of the calculated parameters in Table 1, which is structured as follows: the first columns has the number of clouds, the second and third columns have the velocity shifts of the corresponding blue and red components of each doublet, the fourth and fifth columns have the FWHM (in km/s) of the corresponding blue and red components of each doublet respectively, the sixth and seventh column have the optical depths at line center of the corresponding blue and red components of each doublet respectively.

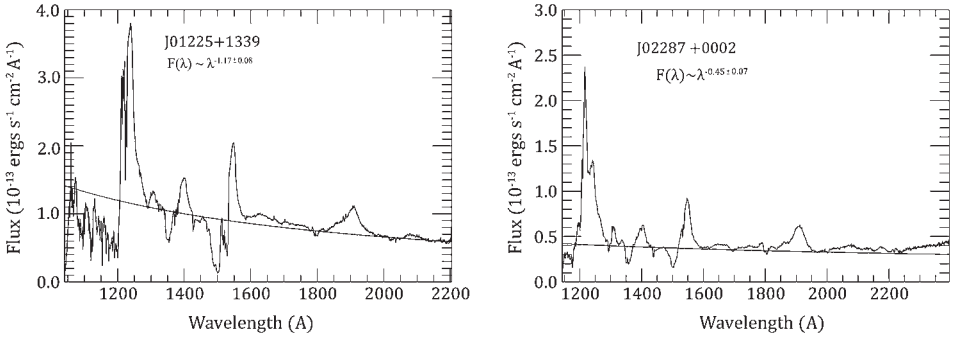

Figure 3. Continuum fits to the spectra of J01225+1339 and J02287+0002. The fitting windows free of strong emission and absorption are given in the text.

Table 1. Calculated parameters obtained by the fitting process.

Cloud	ΔV_b (km/s)	ΔV_r (km/s)	FWHM$_b$ (km/s)	FWHM$_r$ (km/s)	τ_b	τ_r
			J01225+1339			
			Si IV λλ 1393.755, 1402.77 Å			
1	3700±370	3720±370	340±20	340±20	0.16±0.03	0.15±0.03
2	4840±390	4830±390	200±10	200±10	0.29±0.12	0.20±0.08
3	6040±660	6040±650	140±10	140±10	0.10±0.07	0.09±0.06
4	8620±860	8590±860	570±50	570±50	0.23±0.07	0.19±0.06
5	9640±670	9600±670	1160±80	1160±80	0.50±0.20	0.41±0.16
6	10780±850	10780±850	790±60	790±60	0.28±0.10	0.14±0.06
7	12410±620	12370±620	9300±40	930±40	0.11±0.03	0.10±0.03
8	13620±1090	13510±1080	550±40	550±40	0.10±0.03	0.09±0.02
9	15630±780	15680±790	630±30	630±30	0.13±0.03	0.09±0.02
			C IV λλ 1548.187, 1550.772 Å			
1	3800±380	3780±380	530±50	530±50	1.05±0.16	0.92±0.28
2	4960±400	4880±400	330±30	330±30	0.71±0.16	0.49±0.11
3	6180±690	6180±690	210±10	210±10	0.72±0.14	0.66±0.17
4	8550±850	8550±850	900±90	900±90	0.40±0.07	0.33±0.07
5	9730±680	9710±680	1670±110	1670±110	0.64±0.13	0.53±0.11
6	10930±880	10950±880	1190±120	1190±120	0.36±0.11	0.18±0.06
7	12270±610	12230±610	1390±70	1390±70	0.49±0.06	0.44±0.05
8	13730±1100	13620±1100	900±80	900±80	0.30±0.06	0.26±0.03
9	15580±780	15470±780	1020±50	1020±50	0.19±0.02	0.13±0.01
			J02287+0002			
			Si IV λλ 1393.755, 1402.77 Å			
1	860±350	750±300	230±20	230±20	0.12±0.01	0.11±0.01
2	2200±250	2270±300	120±20	120±20	0.11±0.01	0.08±0.01
3	3420±410	3380±440	130±40	130±40	0.11±0.01	0.08±0.01
4	7780±1020	7770±1010	1570±220	1570±210	0.35±0.04	0.32±0.03
5	9450±1110	9400±1200	1500±190	1500±190	0.52±0.06	0.30±0.04
6	11890±1430	11820±1500	830±80	830±80	0.15±0.02	0.10±0.01
7	14540±1790	14540±1890	170±20	170±20	0.05±0.01	0.04±0.01
			C IV λλ 1548.187, 1550.772 Å			
1	970±340	970±310	370±40	370±40	0.10±0.01	0.09±0.01
2	2270±270	2280±280	170±50	170±50	0.48±0.05	0.35±0.05
3	3120±370	3190±380	180±20	180±20	0.42±0.04	0.31±0.04
4	7620±980	7610±980	2220±300	2220±300	0.27±0.02	0.24±0.02
5	9610±960	9550±950	2180±210	2180±210	0.46±0.03	0.27±0.03
6	11820±1360	11750±1350	1270±180	1270±180	0.17±0.01	0.11±0.01
7	13850±1700	13850±1700	280±30	280±30	0.11±0.01	0.09±0.01

The true FWHM is determined considering the instrumental width of the spectrograph, which is 11.1 Å and by using the following equation (Rafiee & Hall 2011):

$$\mathrm{FWHM}^2_{\mathrm{obs}} = \mathrm{FWHM}^2_{\mathrm{true}} + (1+z)^{-2}\mathrm{FWHM}^2_{\mathrm{inst}}, \quad (2)$$

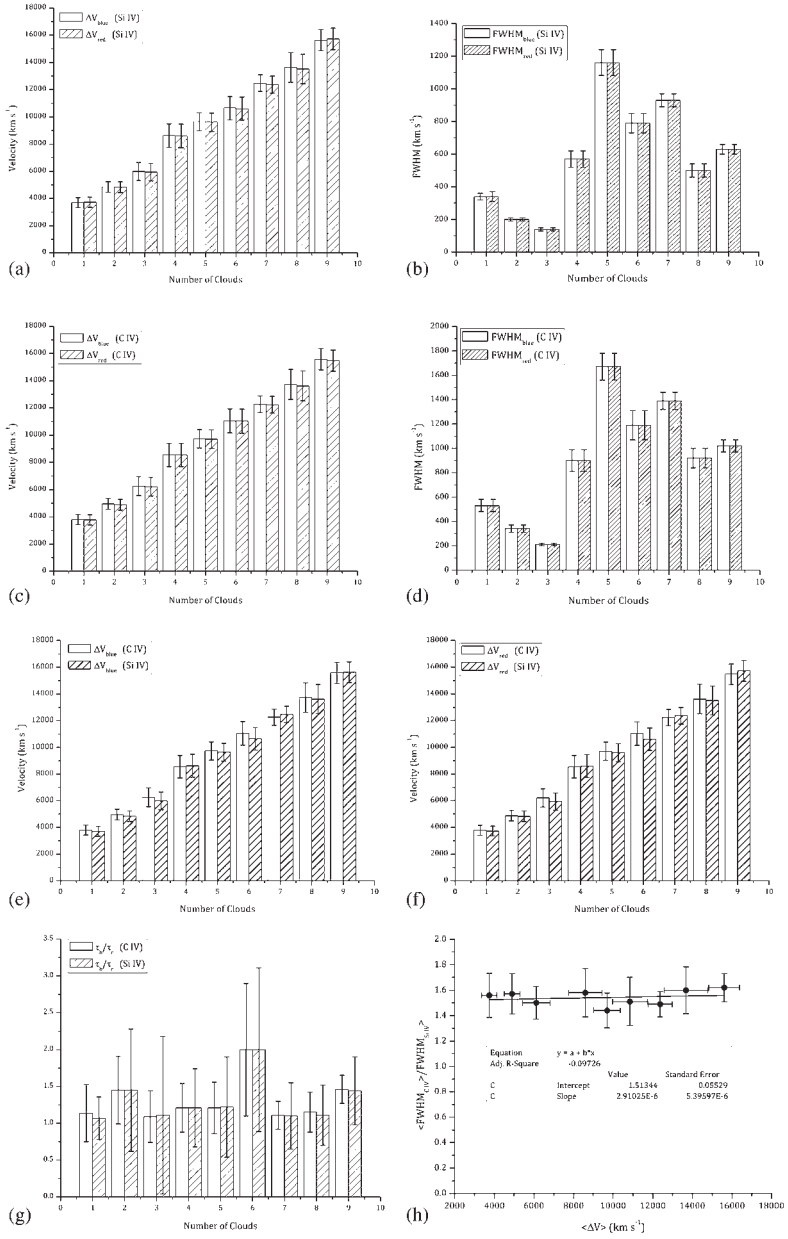

Figure 4. Plotted data for J01225+1339: (**a**) Velocity shifts (ΔV) of Si IV blue (1393.755 Å) and red (1402.77 Å) components of the doublet; (**b**) FWHM of Si IV blue and red components; (**c**) Velocity shifts (ΔV) of C IV blue (1548.187 Å) and red (1550.772 Å) components; (**d**) FWHM of C IV blue and red components; (**e**) Velocity shift of blue components of C IV doublet compared with the velocity shifts of blue components of Si IV doublet; (**f**) Velocity shift of red components of C IV doublet compared with the velocity shifts of red components of Si IV doublet (**g**) optical depth ratio τ_b/τ_r (C IV) compared with the optical depth ratio τ_b/τ_r (Si IV); (**h**) ratio of C IV ⟨FWHM⟩ to Si IV ⟨FWHM⟩ for every cloud as a function of outflow velocity.

where the instrumental broadening ($FWHM_{inst}$) is the observed-frame while the observed ($FWHM_{obs}$) and true ($FWHM_{true}$) full width at half maximum are the rest-frame.

In Fig. 4(a, c) and Fig. 5(a, c), we plot the velocity shifts (ΔV) of the blue and red components of Si IV and C IV for both spectra. From the graphs, it is obvious that the criterion 1(b), stating that the velocity offset of the blue component of a doublet is the same as the velocity shift of the red component, is fulfilled. In Fig. 4(b, d) and Fig. 5(b, d), we give the correlation between the widths of the blue and red components of individual doublets that compose the Si IV and C IV BALs. Again, the criterion 1(c), stating that the width of the blue member of a doublet is the same as the width of the red member is satisfied.

In Figures 4(e) and 5(e), we plot the velocity shifts of the blue components of C IV and the velocity shifts of the blue components of Si IV. In Figures 4(f) and 5(f), we do the same for the red components of C IV and Si IV. As one can see, the criterion 2(b) is satisfied. In Figures 4(g), 5(g) one can observe that the criterion 2(c) is satisfied.

6. Conclusions

In light of the recent observations of Misawa *et al.* (2014) that confirm the existence of clouds, the aim of this study is to propose a method of multicomponent analysis of BAL troughs in the UV spectra of BALQSOs. The main points of our analysis are the following:

(1) We propose a physical model for the structure of BAL material. The broad absorption line region consists of a number of independent clouds where every cloud is a cluster of subunits called cloudlets. In that way we confirmed that the material that composes BAL profiles is in the form of "clouds" rather than a continuous homogenous flow.
(2) Based on the previous consideration we give a possible interpretation for the large widths of BALs. The widths of BALs are caused by the synthesis of broad components produced by clouds. Every component corresponding to a cloud has large width that depends on the internal structure of the cloud which is a cluster of a large number of cloudlets.
(3) We presented the mathematical expression of the physical model. We showed how equation (1) combined with the proposed criteria can decompose the BAL troughs to the exact number of components required to give a unique fit.
(4) We presented a series of criteria that ensure the exact number of components required to achieve a unique fit in the case of the UV resonance lines of Si IV and C IV. The uniqueness of the fit provides a very good estimation of the values of the calculated parameters.
(5) We observed that in both studied spectra, in a group of 16 components (9 components in J01225+1339 and 7 components in J02287+0002) the ratio $FWHM_{CIV}/FWHM_{SiIV}$ has an increasing trend with a mean value of 1.51 ± 0.10 (Figures 4(h), 5(h) and 6).

Fitting Si IV and C IV broad absorption troughs according to the proposed multicomponent analysis method we managed to achieve good fits, (as measured by the

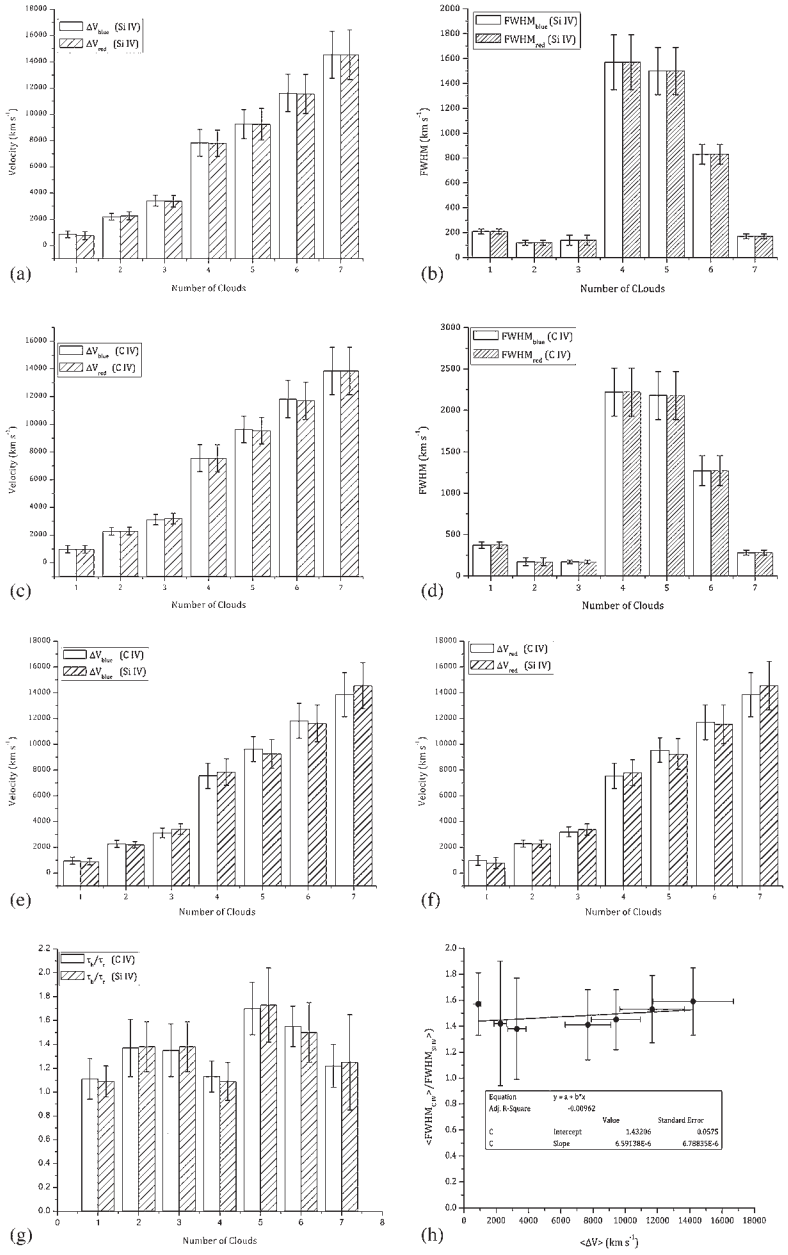

Figure 5. Plotted data for J02287+0002: (**a**) Velocity shifts (ΔV) of Si IV blue (1393.755 Å) and red (1402.77 Å) components of the doublet; (**b**) FWHM of Si IV blue and red components; (**c**) Velocity shifts (ΔV) of C IV blue (1548.187 Å) and red (1550.772 Å) components of the doublet; (**d**) FWHM of C IV blue and red components of the doublet; (**e**) Velocity shift of blue components of C IV doublet compared with the velocity shifts of blue components of Si IV doublet; (**f**) Velocity shift of red components of C IV doublet compared with the velocity shifts of red components of Si IV doublet (**g**) optical depth ratio τ_b/τ_r (C IV) compared with the optical depth ratio τ_b/τ_r (Si IV); (**h**) ratio of C IV FWHM to Si IV FWHM for every cloud as a function of outflow velocity.

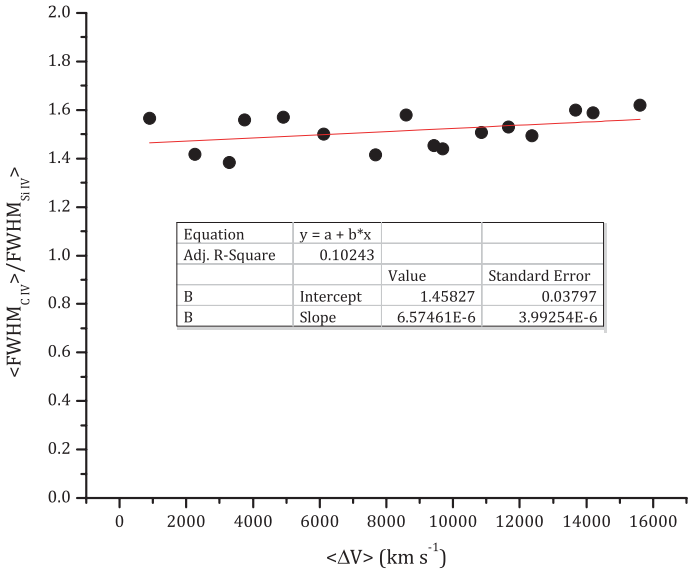

Figure 6. Ratio of C IV FWHM to Si IV FWHM for every component of both BALQSOs as a function of outflow velocity.

reduced χ^2) and show that all the criteria we set are satisfied. In this way we confirm that BAL troughs can be satisfactorily modeled under the assumptions of our proposed method. By applying our multicomponent analysis method in the case of two BALQSO spectra, we calculated the velocity shifts of individual components, the FWHMs and optical depths at line center which are presented in Table 1 and plotted as histograms in Figures 4, 5.

In a future work we would like to study the ratio of parameters between Si IV and C IV components. However, our sample of two BALQSOs is very small, so in order to reach to more robust conclusions about the FWHMs and other parameters we need to study a greater number of BALQSOs. If our conclusions are valid in a larger sample, only then we can reach to some generalized conclusions concerning BALQSOs.

Acknowledgements

This research project is progressing at the University of Athens, Department of Astrophysics, Astronomy and Mechanics, under the financial support of the Ted and Erica Spyropoulos Foundation and the Special Account for Research Grants, which we thank very much. Finally, we would like to thank Prof. Jack Sulentic and Prof. Paola Marziani for kindly providing us with both VLT BALQSO spectra as well as for their useful and detailed comments on our work.

References

Appenzeller, I. *et al.* 1998, *The Messenger*, **94**, 1.
Arav, N., Barlow, T. A., Laor, A., Blandford, R. D. 1997, *MNRAS*, **288**, 1015.

Arav, N., Barlow, T. A., Laor, A., Sargent, W. L. W., Blandford, R. D. 1998, *MNRAS*, **297**, 990.
Bates, B., Gilheany, S. 1990, *MNRAS*, **243**, 320.
Becker, G. D., Rauch, M., Sargent, W. L. W. 2009, *ApJ*, **698**, 1010.
Bottorff, M., Ferland, G. 2000, *MNRAS*, **316**, 103.
Bottorff, M., Ferland, G. 2001, *ApJ*, **549**, 118.
Bottorff, M., Ferland, G. 2002, *ApJ*, **568**, 581.
Bottorff, M., Ferland, G., Baldwin, J., Korista, K. 2000, *ApJ*, **542**, 644.
Capellupo, D. M., Hamann, F., Barlow, T. A. 2014, *MNRAS*, **444**, 1893.
Danezis, E., *The nature of Be stars*, PhD Thesis (University of Athens) (1983).
Danezis, E., Nikolaidis, D., Lyratzi, E., Popović, L. Č., Dimitrijević, M. S., Antoniou, A., Theodosiou, E. 2007, *PASJ*, **59**, 827.
Danezis, E., Nikolaidis, D., Lyratzi, V., Stathopoulou, M., Theodossiou, E., Kosionidis, A., Drakopoulos, C., Christou, G., Koutsouris, P. 2003, *Ap&SS*, **284**, 1119.
de Kool, M., Becker, R. H., Gregg, M. D., White, R. L., Arav, N. 2002, *ApJ*, **567**, 58.
Dietrich, M., Wagner, S. J., Courvoiser, T. J.-L., Bock, H., North, P. 1999, *A&A*, **351**, 31.
Elvis, M. 2000, *ApJ*, **545**, 63.
Farrah, D. *et al.* 2012, *ApJ*, **745**, 178.
Farrah, D., Urrutia, T., Lacy, M., Lebouteiller, V., Spoon, H. W. W., Bernard-Salas, J., Connolly, N., Afonso, J., Connolly, B., Houck, J. 2010, *ApJ*, **717**, 868.
Filiz Ak, N. *et al.* 2012, *ApJ*, **757**, 114.
Filiz Ak, N. *et al.* 2014, *ApJ*, **791**, 88.
Foltz, C. B., Chaffee, F. H., Hewett, P. C., Weymann, R. J., Morris, S. L. 1990, *BAAS*, **2**, 806.
Foltz, C., Wilkes, B., Weymann, R., Turnshek, D. 1983, *PASP*, **95**, 341.
Gibson, R. R., Jiang, L., Brandt, W. N. *et al.* 2009, *ApJ*, **692**, 758.
Gilheany, S. *et al.* 1990, *Ap&SS*, **169**, 85.
Gonçalves, D. R., Friaça, A. C. S., Jatenco-Pereira, V. 2001, *MNRAS*, **328**, 409.
Hall, P. B. *et al.* 2013, *MNRAS*, **434**, 222.
Hamann, F., Chartas, G., McGraw, S., Rodriguez Hidalgo, P., Shields, J., Capellupo, D., Charlton, J., Eracleous, M. 2013, *MNRAS*, **435**, 133.
Hazard, C., McMahon, R. G., Webb, J. K., Morton, D. C. 1987, *ApJ*, **323**, 263.
Hewett, P. C, Foltz, C. B. 1784, *AJ*, 125.
Laor, A., Bahcall, J. N., Jannuzi, B. T., Schneider, D. P., Green, R. F, Hartig, G. F. 1994, *ApJ*, **420**, 110.
Lyratzi, E., Danezis, E., Popović, L. Č., Antoniou, A., Dimitrijević, M. S., Stathopoulos, D. 2011, *BaltA*, **20**, 448.
Lyratzi, E., Danezis, E., Popović, L. Č., Dimitrijević, M. S., Antoniou, A., Stathopoulos, D. 2010, *MSAIS*, **15**, 161.
Lyratzi, E., Danezis, E., Popović, L. Č., Dimitrijević, M. S., Nikolaidis, D., Antoniou, A. 2007, *PASJ*, **59**, 357.
Lyratzi, E., Popović, L. Č., Danezis, E., Dimitrijević, M. S., Antoniou, A. 2009, *NewAR*, **53**, 179.
Markova, N. 2000, *A&AS*, **144**, 391.
McKee, C. F., Tarter, C. B. 1975, *ApJ*, **202**, 306.
Misawa, T., Inada, N., Oguri, M., Gandhi, P., Horiuchi, T., Koyamada, S., Okamoto, R. 2014, *ApJ*, **794**, 20.
Murray, N., Chiang, J. 1995, *ApJ*, **454**, 105.
Murray, N., Chiang, J., Grossman, S. A., Voit, G. M. 1995, *ApJ*, **451**, 498.
Negrete, A., Dultzin, D., Marziani, P., Sulentic, J. W. *et al.* 2014, *ApJ*, **794**, 95.
Proga, D., Stone, J. M., Kallman, T. R. 2000, *ApJ*, **543**, 686.
Rafiee, A., Hall, P. B. 2011, *ApJS*, **194**, 42.
Reichard, T. A., Richards, G. T., Hall, P. B., Schneider, D. P., VandenBerk, D. E., Fan, X., York, D. G., Knapp, G. R., Brinkmann, J. 2003, *AJ*, **126**, 2594.

Rivinius, T. *et al.* 1997, *A&A*, **318**, 819.
Savage, B. D., Sembach, K. R. 1991, *ApJ*, **379**, 245.
Takeuchi, S., Ohsuga, K., Mineshige, S. 2013, *PASJ*, **65**, 88.
Trump, J. R. *et al.* 2006, *ApJS*, **165**, 1.
Turnshek, D. A. 1984, *ApJ*, **280**, 51.
Turnshek, D. A. 1988, in: *QSO Absorption Lines: Probing the Universe*, edited by Blades, J. C., Norman, C., Turnshek, D. A. (Cambridge: Cambridge Univ Press), p. 17.
Turnshek, D. A., Grillmair, C. J., Foltz, C. B., Weymann, R. J. 1988, *ApJ*, **325**, 651.
Urrutia, T., Becker, R. H., White, R. L., Glikman, E., Lacy, M., Hodge, J, Gregg, M. D. 2009, *ApJ*, **698**, 1095.
Voit, G. M., Weymann, R. J., Korista, K. T. 1993, *ApJ*, **413**, 95.
Waldron, W. L., Klein, L., Altner, B. 1992, *ASP Conf. Series*, **22**, 181.
Weymann, R. J., Morris, S. L., Foltz, C. B., Hewett, P. C. 1991, *ApJ*, **373**, 23.
Weymann, R. J., Turnshek, D. A., Christiansen, W. A. 1985, in: *Astrophysics of active galaxies and quasi-stellar objects, broad absorption line quasars (BALQSOs)*, edited by Miller J. S. (University Science Books, Mill Valley, CA), p. 333.
Wildy, C., Goad, M. R., Allen, J. T. 2015, *MNRAS*, **448**, 2397.